analytical chemistry

Editors' Highlight

pubs.acs.org/ac

Ion Sponge: A 3-Dimentional Array of Quadrupole Ion Traps for Trapping and Mass-Selectively Processing Ions in Gas Phase

Wei Xu,[†,#] Linfan Li,[‡,#] Xiaoyu Zhou,[‡] and Zheng Ouyang*[,‡]

[†]School of Life Science, Beijing Institute of Technology, Beijing, 100081, China

[‡]Weldon School of Biomedical Engineering, Purdue University, West Lafayette, Indiana 47907, United States

Supporting Information

ABSTRACT: In this study, the concept of ion sponge has been explored for developing 3D arrays of large numbers of ion traps but with simple configurations. An ion sponge device with 484 trapping units in a volume of 10 × 10 × 3.2 cm has been constructed by simply stacking 9 meshes together. A single rf was used for trapping ions and mass-selective ion processing. The ion sponge provides a large trapping capacity and is highly transparent for transfer of ions, neutrals, and photons for gas phase ion processing. Multiple layers of quadrupole ion traps, with 121 trapping units in each layer, can operate as a single device for MS or MS/MS analysis, or as a series of mass-selective trapping devices with interlayer ion transfers facilitated by AC and DC voltages. Automatic sorting of ions to different trapping layers based on their mass-to-charge (m/z) ratios was achieved with traps of different sizes. Tandem-in-space MS/MS has also been demonstrated with precursor ions and fragment ions trapped in separate locations.

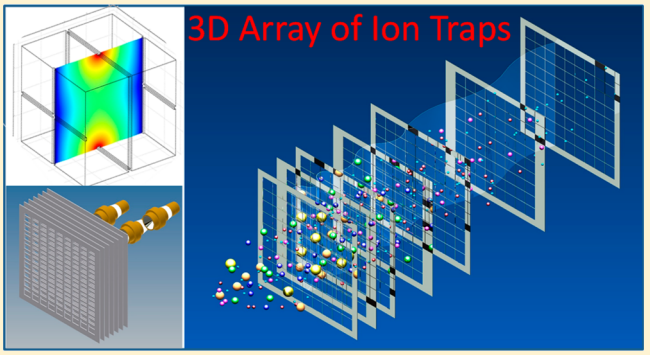

Quadrupole ion trap has compact size and simple configuration. It is suitable for tandem mass spectrometry analysis with a single analyzer.[1] The relatively high operation pressure is also good for efficient CID (collision induced association) and implementation for miniature mass spectrometers with low pumping capacity.[2,3] In addition to the mass analysis, quadrupole ion traps have also been widely used for ion processing in hybrid instruments and can be coupled with quadrupole filters,[4] a Fourier transform ion cyclotron resonance (FTICR) cell,[5] Orbitrap,[6] and time-of-flight (TOF) mass analyzers.[7] Arrays of ion traps have also been explored previously, mainly for two purposes: (I) to compensate for the trapping capacity reduced with miniature ion traps[8−11] or (II) to perform multichannel mass analysis in parallel for high throughput analysis.[12−14] By shrinking the size of the ion traps, maximum rf amplitude required for covering a same mass-to-charge (m/z) range is reduced and therefore low-power and small-size electronics can be used. The miniaturized ion traps, however, could suffer from severe space charge effect. Two-dimension arrays of miniature cylindrical ion traps have been built to enlarge the total space for trapping, with the number of traps ranging from a few[13] to several hundreds[10] or one million.[11] Use of micro fabrication methods[10,11] was necessary for constructing the arrays with a large number of ion traps of micrometer sizes. Arrays of linear ion traps have also been made,[9,15] but the production of arrays with large numbers of trapping units is very difficult due to the complexity in the configuration of a linear ion trap. Using the virtual electrode approaches, linear arrays of rectilinear ion traps[8] and arrays of halo ion traps[16] have been developed with relatively low structural complexity.

In this study, we have explored a method of constructing ion trap arrays of large capacities but with extremely simple configurations, which therefore are also very easy to fabricate. Meshes with narrow wires were used to construct a 3D array with hundreds of ion traps in multiple layers. This device is named as "ion sponge". The array is highly transparent, suitable for injection of gas phase particles into different layers of the device as well as for the ion transfers among the layers. The ions can be stored, mass selectively isolated, sorted, and transferred for various tandem mass spectrometry processes.

DESIGN OF 3D ARRAY OF ION TRAPS AND PERFORMANCE OPTIMIZATION

A proof-of-concept design of the ion sponge is illustrated in Figure 1a. A number of stainless steel meshes, made by wire EDM (electrical discharge machining, Allied Precision Machine Inc., Lafayette, IN), were stacked together with an interplate distance of z_0 to construct the trap array. Each mesh of a thickness t had a large number of square holes of an identical size of $2r_0 \times 2r_0$ and a wire width of t. The centers of the holes were aligned for every other meshes but with a shift between each adjacent two (Figure 1b). A single rf was applied on all the meshes of even numbers, which made each of the square holes

Received: March 1, 2014
Accepted: April 23, 2014
Published: April 23, 2014

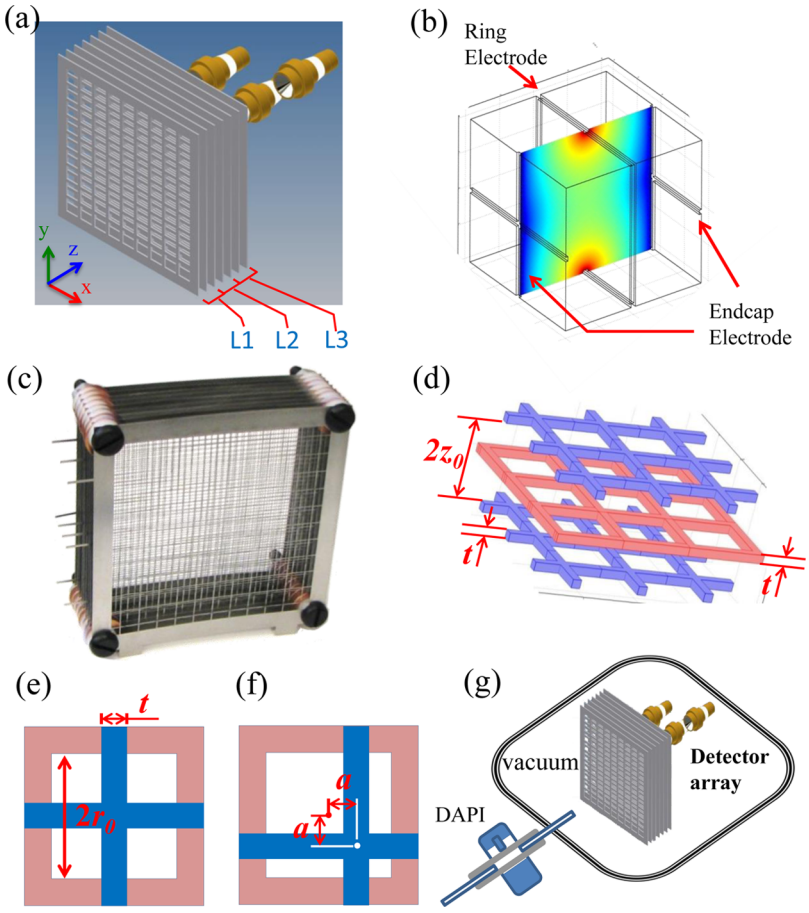

Figure 1. (a) 3D mechanical drawing of an ion sponge with three trapping layers. Ions detected with three electron multipliers. (b) Schematic configuration of a single trapping unit, with a square ring electrode and two cross end-cap electrodes, and simulated electric field. (c) Photo of an ion sponge with four trapping layers. (d) Schematic configuration of 1 trap layer and geometries (e) without and (f) with a shift of the cross end-cap electrodes off the center of the square hole. (g) Schematic instrument setup for testing, with a DAPI interface for directly introducing ions from ion sources in an ambient environment.

acting as the ring in a traditional 3D quadrupole ion trap. The crosses of the wires on meshes of odd numbers acted as the end-cap electrodes of the ion traps, on which the AC or DC signals were applied to manipulate the ions trapped in each layer. One of the many trapping units is shown in Figure 1b, with two metal crosses from the two odd-numbered meshes as the end-cap electrodes and a square metal frame from an even-numbered mesh as the ring electrode. Each end-cap electrode mesh was shared by two adjacent layers of ion traps. Therefore, each additional trap layer could be added with two additional meshes. An array made with 9 meshes is shown in Figure 1c, with 4 layers of a total of 484 ion traps in a volume of 10 × 10 × 3.2 cm. The dimensions of the trapping units, including the trap width $2r_0$, the interend-cap distance $2z_0$, and the electrode width t, are defined as shown in Figure 1d,e.

As expected, each of the trapping units in the ion sponge would have a highly distorted quadrupolar field in comparison with the Paul trap. The field solved using COMSOL (V. 4.3, COMSOL, Inc., Burlington, MA) for one trapping unit with an rf voltage on the ring electrode is shown in Figure 1b. The shape of the electric field is still similar to a traditional 3D quadrupole ion trap, and the trapping of ions is expected to occur with a dynamic rf field of proper amplitude applied. The following equation should still be applicable for the traps in an ion sponge:

$$q = A_2 \frac{4eV}{mr^2\Omega^2}$$

where q is the Mathieu parameter, A_2 is the quadrupole coefficient, V and Ω are the rf amplitude and frequency, respectively, and m and e are the molecular weight and charge, respectively, of the ion. As for cylindrical[17] and rectilinear[18] ion traps with simplified and imperfect geometries, the quadrupole coefficient A_2 is expected to be relatively small for the traps in an ion sponge due to the stronger high-order fields.[19]

The purpose for the development of an ion sponge device is to explore alternative means for trapping and manipulating a large number of ions for multistage ion processing in gas phase. Achieving high resolution for MS analysis is not the primary goal in this study. However, understanding the geometric effect on the mass selective processes, such as ion isolation and the ion transfer, would be of great interest for future implementation of this type of device. Ion sponges of different dimensions were designed with assistance of numerical simulations of ion trajectories using a method previously reported[20] (see Supporting Information for details). Geometry optimization was made with considerations of trapping efficiency, intertrap ion transfer efficiency, and mass selectivity or mass resolution, while keeping the simplicity of the device configuration. The geometries evaluated are listed in Table 1. For some of them, the crosses of both end-cap electrodes were

dx.doi.org/10.1021/ac5008046 | Anal. Chem. 2014, 86, 4102−4109

Table 1. Six Geometries Used in the Study of the Ion Sponge[a]

trap geometry	r_0 (mm)	z_0 (mm)	t (mm)	a (mm)
I	2.62	2.75	0.76	0
II	3.88	3.75	0.25	0.13
III	2.88	2.75	0.25	0.13
IV	3.88	3.20	0.25	0.13
V	3.88	6.40	0.25	0.13
VI	3.88	3.75	0.25	0

[a]See Figure S1, Supporting Information, for definition of dimensions.

shifted by a distance of a in both x and y directions from the center axis of the square ring electrode, which was expected to allow better transfer of the ions between layers of ion traps. As shown in Figure S1a,b, Supporting Information, with the simulated spectra for Geometry I and VI, a decrease in the wire width resulted in an improvement in the mass resolution, e.g., from $\Delta m/z$ of about 3 at half-maximum of the peak for Geometry I to about 1.8 for Geometry VI. This is most likely due to a smoother virtual electric surface formed with the narrower electrodes. In Geometry II (Table 1 and Figure S1c, Supporting Information), the cross electrode was moved off the center by 0.13 mm and a higher efficiency for ion transferring out of the ion trap by rf scan could be obtained. A resolution similar to Geometry VI was obtained. The ratios of high-order field components (octopole A_4 and dodecapole A_6) over quadrupole field A_2 inside a single trapping cell are $A_4/A_2 = -0.199$ and $A_6/A_2 = 0.303$, respectively (see Supporting Information for calculation of A_2, A_4, and A_6).

During the characterization of the ion sponge performance (to be further discussed later), it was found that the trapping efficiency for the last trap layer next to the electron multiplier was very low, which was due to the field penetration by the high DC voltage applied on the electron multiplier. The last two meshes of each ion sponge were thereby grounded for shielding. For the low-voltage signals applied on cross electrodes for ion excitation or isolation in selected trap layers (to be further described later), no significant effect due to field penetration was observed. The ion sponges of different geometries constructed for experimental characterization all had 121 trapping units on each layer.

EXPERIMENTAL SECTION

The ion sponges were characterized using a home-built testing system[21] (Figures 1g and S3a, Supporting Information) that had a single-stage vacuum chamber. A discontinuous atmospheric pressure interface (DAPI)[22] was used for transferring ions from an atmosphere pressure ionization source. The ion sponge was placed in the vacuum chamber behind the DAPI inlet capillary (Figure S2b, Supporting Information). Three electron multipliers were mounted on a print circuit board to detect the ions ejected from different locations of the trap array (Figure S2c, Supporting Information). Ion intensities detected by these detectors were representative for ions ejected from the center, horizontal edge, and vertical edge of the ion sponge. The spectra shown in this manuscript were recorded using the electron multiplier 2 (Figure S2c, Supporting Information) located at the center, unless otherwise specified. Details of the control system have been previously described.[21] The frequency of the rf applied on the ring electrodes was 820 kHz with a typical amplitude of about 112 $V_{0\text{-}p}$ for trapping the ions during the DAPI open period, unless otherwise specified.

Different ionization sources were used in the experiments to generate ions, including nanoelectrospray ionization (nano-ESI), using glass capillaries each with a pulled tip, and atmosphere pressure chemical ionization (APCI) using a corona discharge. For experiments using multiple beam of ions or gas molecules, multiple DAPIs were used with bent capillaries[23] for a convenient implementation. Cocaine, *N,N*-diethyl-3-methylbenzamide (DEET), *p*-bromo-benzoic acid, and diethyl-methoxy-borane were purchased from Sigma Chemical Co. (Sigma-Aldrich, St. Louis, MO). MRFA (Met-Arg-Phe-Ala) was purchased from Research Plus Inc. (Manasquan, NJ). Imatinib was purchased from Santa Cruz Biotechnology Inc. (Santa Cruz, CA). Samples used with nanoESI (cocaine, MRFA, *p*-bromo-benzoic acid, imatinib) were prepared in a methanol/water solution (1:1 v/v).

MASS-SELECTIVE ION EJECTION

Mass-selective ejection of the ions out of the ion sponge was experimentally characterized for Geometry I and II (Table 1) for a comparison. The ion sponge of each geometry had 3 layers of ion traps constructed with 9 meshes (last two grounded for shielding). Mass selective instability scan was performed by increasing the rf amplitude while recording the ion signals using the central detector. Spectra were recorded for MRFA and DEET ionized by nanoESI and APCI, respectively. The ions were introduced through DAPI and trapped in the ion trap array. With a delay of 500 ms after the DAPI closing, the ions were mass selectively analyzed by scanning the rf amplitude at a rate of about 4000 Da/s. A resonance ejection condition was established by applying the opposite phases of an AC signal (376 kHz) alternatingly on the odd-numbered meshes. The amplitude of AC was also ramped from 1.0 to 1.2 V along with the rf scan. For the protonated ions, m/z 525 from MRFA and m/z 192 from DEET, and the proton-bound dimer of DEET m/z 383, the mass resolution was found to be better with Geometry II (Figure 2). For instance, $\Delta m/z$ of 1.9 was obtained at the half-maximum of the peak, in comparison with 2.4 for Geometry I. The resolution for Geometry II is similar to the simulated $\Delta m/z$ of ~1.8 (Figure S1c, Supporting Information), and the resolution improvement with the narrower electrodes is in agreement with the observation from the simulations.

The mass resolution of an ion trap array is affected by the resolving power of each individual ion trap as well as the consistency in dimensions of all the trap units. As demonstrated previously, the mass shifts among traps due to imperfect fabrication could contribute to the broadening of the peaks observed with the entire array.[24] This effect was tested by comparing the resolutions of the spectra obtained with the entire array or an individual channel (with only a small area exposed to ion detector). However, no significant difference was observed, presumably because the dimension of every trapping unit was large in comparison with the fabrication imperfections; also the resolution of individual unit was already compromised due to the distorted field associated with the simple configuration.

DISTRIBUTION OF THE TRAPPED IONS

The sensitivity for the mass analysis using the ion sponge is dependent on the efficiency of trapping the ions introduced and the open period of the DAPI, which is typically shorter than 20 ms to avoid elevation of pressure above 500 mTorr in the

dx.doi.org/10.1021/ac5008046 | Anal. Chem. 2014, 86, 4102−4109

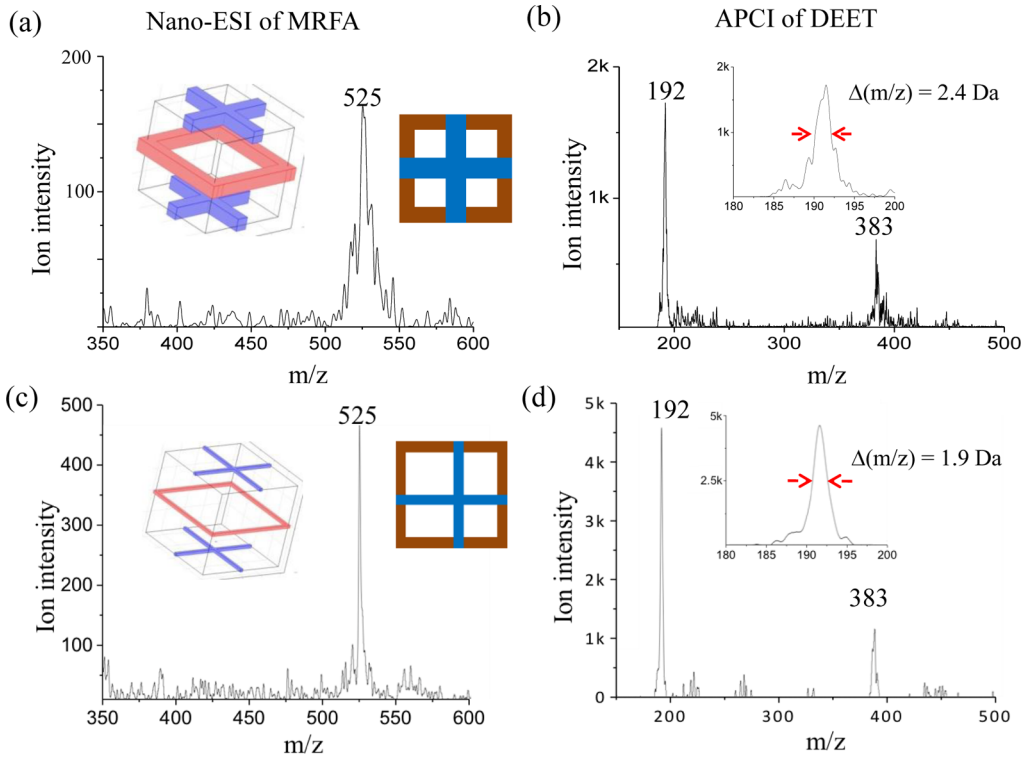

Figure 2. Mass spectra of MRFA (a and c) and DEET (b and d) obtained from ion sponges of Geometry I (a and b) and II (c and d), resonance ejection at 376 kHz.

manifold. Every individual ion trap inside the array is a 3D quadrupole ion trap. While the efficiency for trapping externally injected ions is typically very low for individual 3D ion traps,[25,26] the 3D array of 3D traps is expected to have an improved overall efficiency for catching the ions introduced by DAPI. The distributions of the ions trapped in an ion sponge were characterized in the following two experiments.

An ion sponge of Geometry I with 2 trap layers (7 meshes) was used in a study with simultaneous ion injections at different locations (Figure S3a, Supporting Information). The cocaine ions and DEET ions, generated by nanoESI and APCI, respectively, were introduced toward the ion sponge at the same time using two DAPIs. The signal intensities for the protonated cocaine m/z 304 and DEET dimer m/z 383 were recorded by the three detectors during the mass selective instability scans as shown in Figure S3b, Supporting Information, which reflects the distributions of these ions in the XY plane of the ion sponge. It was obvious that these two types of ions were trapped in the space with relatively broad distributions, centered at the points of injection but overlapping with each other.

The broadening of the ion distribution was further characterized by varying the distance between the center DAPI capillary and the ion sponge (Figure S4a, Supporting Information). Since there was a gas expansion after the DAPI inlet,[27] more broadened distributions would have been expected for longer distances; however, it was actually observed with the shortest distance of 2.5 mm (Figure S4b, Supporting Information). The vacuum pressure varies during the DAPI open time and can increase to several hundred millitorrs. The local pressure at the first mesh in this case, for example, with a background vacuum pressure of 100 mTorr, was calculated to be about 10 Torr based on the data extracted from the simulations previously reported,[27] corresponding to a mean free path of about 5.3 μm. A strong disturbance of the gas jet can be caused with the cross electrodes on the first mesh of the ion sponge, which facilitated the dispersion of the ion laterally into traps located far from the center in the XY plane.

Besides the lateral distribution of ions in the XY plane, the ion distribution along the Z direction could also be characterized layer by layer. This could be easily done by eliminating the ions in some of the layers prior to scanning the ions trapped in other layers. The elimination of the ions trapped in the two adjacent layers was achieved by applying a broadband SWIFT on the shared end-cap electrode. Trapping of the ions ejected by SWIFT from one layer into other layers was not observed in our experiments, which presumably was due to the relatively high kinetic energies gained by the ions during the resonance excitation. The disturbance to the ion trapping in the last layer by the high voltage on the detectors was observed with this type of characterization. For a three-layer ion sponge, no mass shift was observed for ions ejected from different layers of the ion sponge, which means the effect due to a difference in the time-of-flight for passing through the meshes was minimal.

In order to distinguish the original trapping layers for the ions detected in a single scan, resonance ejection was implemented with a different ejection point set for each layer. For example, using an ion sponge of Geometry I with two trapping layers (noted as L1 and L2, Figure S5a, Supporting Information), the boundary ejection can be used for layer L1 while a resonance ejection can be used for layer L2 (Figure S5b, Supporting Information). For the experimental demonstration, a monopolar AC signal (AC frequency 290 kHz, 1.5 V) was applied on the mesh number 5 (Figure S5a, Supporting Information) during the mass selectively instability scan. Ions trapped in L2 were ejected earlier than those of the same m/z values but trapped in L1. The spectra recorded for DEET

dx.doi.org/10.1021/ac5008046 | Anal. Chem. 2014, 86, 4102−4109

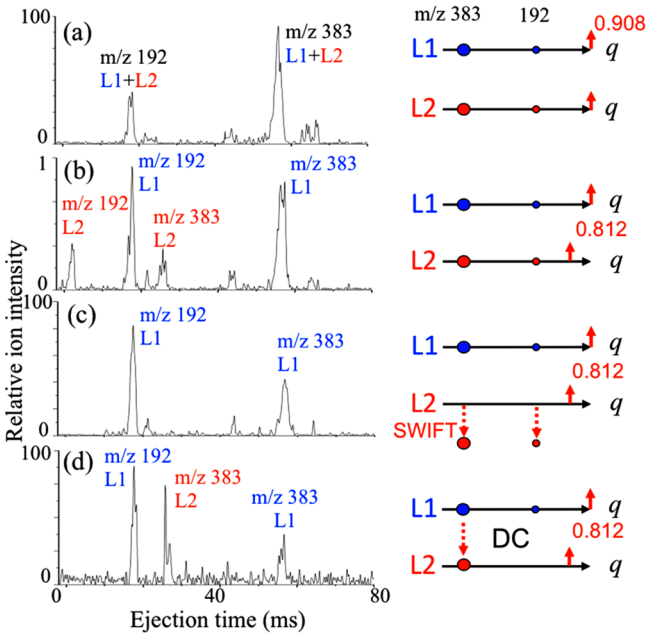

Figure 3. Mass spectra of DEET (a) with boundary ejections for both layers L1 and L2 and (b) with boundary ejection for L1 and resonance ejection for L2. (c) Mass spectrum of DEET recorded with boundary ejection for L1, after ions in L2 eliminated by applying a SWIFT. (d) Mass spectrum of DEET after ion transfer from L1 to L2 using DC pulses, boundary ejection for L1, and resonance ejection for L2.

without and with the resonance ejection for L2 are shown in Figure 3a,b, respectively. Two peaks, for the protonated ion m/z 192 and proton-bound dimer m/z 383, were observed with the boundary ejections for both layers. However, two additional peaks appeared with the resonance ejection applied on L2 (Figure 3b), corresponding to the m/z 192 and m/z 383 ejected at a lower q from L2. The layers of origins for the peaks were confirmed by the pre-elimination method described above. This differential ejection method of shifting peaks for different layers using resonance ejections was applied as a general means for characterizing the ions trapped in different layers after each procedure for gas phase ion processing.

Inter-Layer Ion Transfer. The ion transfer from L1 to L2 was performed using the same ion sponge and subsequently characterized using the resonance ejection method described above. After the DEET ions were introduced into the two layers of the ion sponge, layer L2 was emptied by applying a broadband SWIFT (frequency range 10−410 kHz, amplitude 5 V, duration 50 ms) on mesh No. 5 (Figure S5a, Supporting Information). The spectrum recorded with an rf scan is shown in Figure 3c, showing the ions ejected from L1 with a boundary ejection. To transfer ions from L1 to L2, a DC pulse of 1 ms and 110 V was applied on the mesh No. 1 to push the ions toward the L2. It was found that it was necessary to apply a DC pulse on mesh No. 5 simultaneously, with an optimized voltage of 30 V, to catch the ions in L2. A similar procedure was used in a previous study for ion transfer between two cylindrical ion traps.[28] Figure 3d shows a MS spectrum recorded with resonance ejection for L2 after the ion transfer. The peak of m/z 383 reappeared for L2, indicating a successful transfer of some proton-bound dimers from L1 to L2. The scan function for implementing the experiment is shown in the Supporting Information (Figure S6).

Mass Selective Ion Sorting. Another interesting function developed with the ion sponges is the mass selective ion sorting, which enabled an automatic separation of ions in gas phase based on their m/z values. The implementation of this

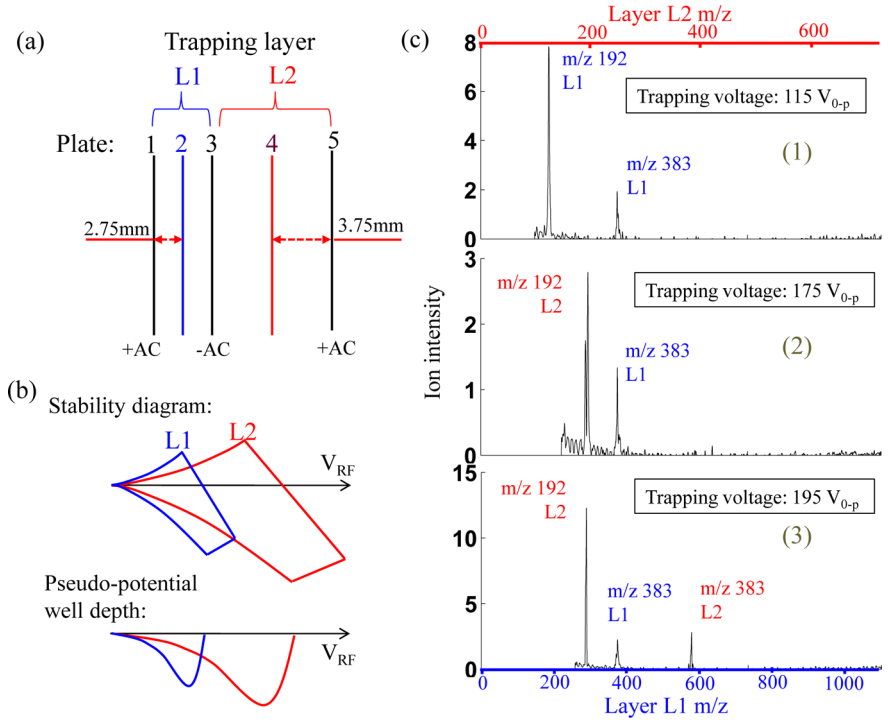

Figure 4. (a) Schematic configuration of an ion sponge with two layers of different sizes and (b) corresponding illustrations of the conceptual stability diagrams and pseudopotential well depths with the same RF applied on both layers. (c) Mass spectra obtained for DEET ions using an ion sponge with Geometry III for L1 and Geometry II for L2 with trapping rf amplitude of 115 $V_{0\text{-}p}$, 175 $V_{0\text{-}p}$, and 195 $V_{0\text{-}p}$.

dx.doi.org/10.1021/ac5008046 | Anal. Chem. 2014, 86, 4102−4109

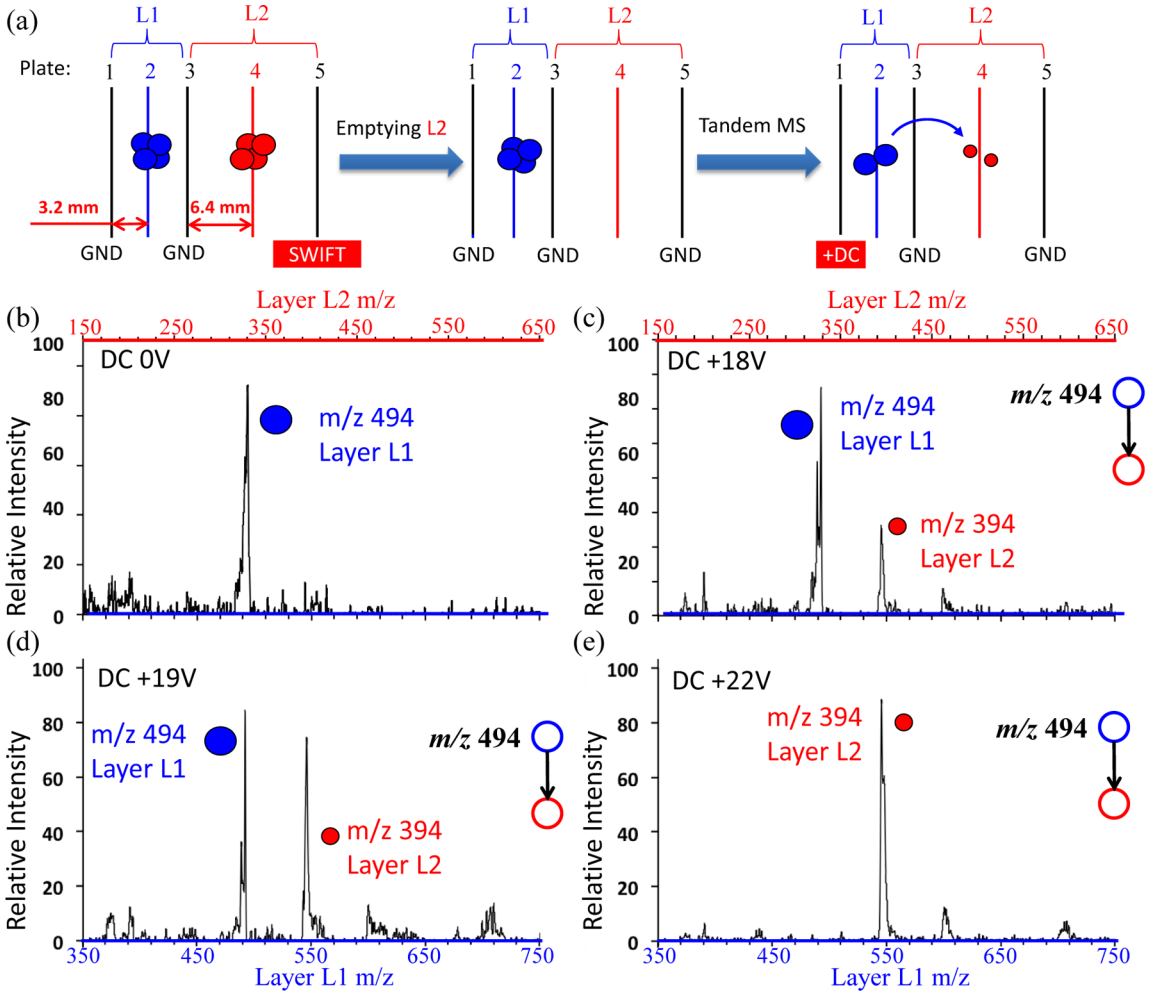

Figure 5. (a) Schematic illustration of the tandem-in-space procedure for an ion sponge with two trap layers of different sizes. (b–e) Mass spectra recorded for CID of protonated imatinib m/z 494 using an ion sponge with L1 of Geometry IV and L2 of Geometry V, at activation DC voltage of (b) 0 V, (c) +18 V, (d) +19 V, and (e) +22 V DC, respectively.

concept is based on the creation of a different potential well depth for each layer in an ion sponge, optimized for ions of a narrow m/z range. The potential well depth for ions of a particular m/z value in an ion trap is dependent on the trap size.[1,29] By adjusting the trap geometry of each layer (Figure 4a), the stability diagrams and potential well depths could become different even though the same rf is applied on ring electrode meshes of all the layers (Figure 4b). A series of ion transfer experiments were carried out using a 2-layer ion sponge (7 meshes), with layer L1 of Geometry III (smaller) and L2 of Geometry II (larger) (Figure 4a). The DEET ions were introduced through DAPI into this ion sponge. The trapped ions were scanned out with boundary ejection for L1 and resonance ejection for L2. As shown in Figure 4c, when a relatively low RF trapping voltage (115 $V_{0\text{-}p}$) was applied during the ion injection, the protonated DEET monomer m/z 192 and dimer m/z 383 could only be trapped in L1 but not in L2. As the amplitude of the trapping rf increased to 175 $V_{0\text{-}p}$, the DEET monomer ions m/z 192 were trapped in L2 while the dimer ions m/z 383 were only trapped in L1. Further increase of the rf voltage to 195 $V_{0\text{-}p}$ enabled the trapping of both DEET monomer and dimer ions in L2, while only dimer ions trapped in L1. This interesting feature of the ion sponges could be used for mass-selective accumulation of ions in different locations in an ion sponge, which can be dynamically adjusted in real time with the trapping rf voltage. The adverse space charge effect to ions of low abundance could potentially be minimized using this method.

Tandem Mass Spectrometry in Space. Tandem mass spectrometry (MS/MS) is a powerful tool in chemical analysis and study of gas phase ion chemistry. It can be used to eliminate the background chemical noise and to elucidate the chemical structures of the compounds. MS/MS can be easily performed using an ion sponge by applying the notched SWIFT for ion isolation followed by an excitation AC for CID. In our experiments, these signals were applied to the shared end-cap meshes and CID occurred simultaneously in all the trapping units (see Figures S7 and S8, Supporting Information). In this "tandem-in-time" mode, the fragment ions were produced and trapped in the same trap unit where the precursor ions were trapped and isolated, just like using a single quadrupole ion trap.[1]

Using the multilayer feature of the ion sponge, a "tandem-in-space" mode was also developed. The tandem-in-space analysis is typically performed using instruments with beam type CID, such as a triple quadrupole, quadrupole-quadrupole-trap, or quadrupole-TOF (time-of-flight) instruments. The precursor isolation, ion fragmentation, and fragment ion analysis are performed in different analyzers. In comparison with a tandem-in-time procedure in a single ion trap, one of the advantages of

dx.doi.org/10.1021/ac5008046 | Anal. Chem. 2014, 86, 4102–4109

tandem in space is the reduction of the space charge effect on the fragment ions of interest. The fragment ions can also be continuously accumulated as in a QTrap instrument (AB Sciex, Toronto, Canada).[4] While the multiple layers of ion traps in an ion sponge can be all operated uniformly in a parallel fashion, they can also be used as multiple stages of analyzers in a sequential fashion to implement the tandem-in-space procedure. For an ion sponge with layers of different sizes similar to that shown in Figure 4a, the L2 with traps of larger sizes has a stability diagram and a potential well better suited for trapping the fragment ions in a lower m/z range (Figure 4b). In L1, the precursor ions can be set at a high q value for CID with a higher excitation energy. This would not be applicable with the typically tandem-in-time approach using a single ion trap,[30,31] since the fragment ions could not be stably trapped in the same device. However, using the ion sponge with layers of different sizes, the fragment ions could possibly be caught by L2 with a lower low-mass cutoff at the same rf voltage.

For experimental implementation, an ion sponge of 2 layers was constructed as shown in Figure 5a, with L1 of Geometry IV and L2 of Geometry V with a larger z_0. The protonated imatinib m/z 494 was produced by nanoESI and introduced through the DAPI. The ions trapped in L2 were eliminated by applying a broadband SWIFT on the mesh 5 (Figure 5a). The isolation of the precursor ions in L1 can be done by applying a notched SWIFT on mesh 1 and/or 3. Instead of applying an AC like in a traditional ion trap for CID, a DC voltage was applied on mesh 1, which displaces the trapped ions off the center of the trap and induces the excitement of the ions with the higher RF field.[32−34] The positive DC voltage applied on mesh 1 also pushed the fragment ions toward L2 which facilitated the directional transfer. The actual scan function used for the tandem-in-space procedure is shown in Figure S9, Supporting Information. The differential ejection method was used to examine the ions from both L1 and L2. As shown with the spectra in Figure 5b,c, the CID occurred with a DC voltage of 18 V and the fragment ions were all trapped in L2. The CID efficiency increased at higher DC voltages (Figure 5d), and a complete dissociation of protonated imatinib m/z 494 was achieved at 22 V (Figure 5e).

CONCLUSION

In this study, we have explored a novel concept for constructing trap arrays of large numbers of units with simple means for fabrication. For the first time, we demonstrated the fabrication and the function of a 3-dimentional array of quadrupole ion traps. The ion sponge provides large trapping capacity and is capable of catching externally introduced ions at a maximal efficiency. Flexible operations and versatile procedures, such as interlayer ion transfer, mass-selective ion sorting, or tandem-in-space MS/MS, can be implemented with a single driving rf. A tandem MS device with a large number of stages could be developed by simply adding two meshes for each stage. The ion sponge potentially is best suited for gas phase ion processing prior to a final MS analysis in hybrid mass spectrometers.

ASSOCIATED CONTENT

Supporting Information

Additional information as noted in text. This material is available free of charge via the Internet at http://pubs.acs.org/.

AUTHOR INFORMATION

Corresponding Author

*E-mail: Ouyang@purdue.edu. Phone: 765-494-2214 Fax: 765-496-1912.

Author Contributions

#W.X. and L.L. contributed equally.

Notes

The authors declare no competing financial interest.

ACKNOWLEDGMENTS

This work was supported by National Science Foundation (0847205-CHE), National Institute of General Medical Sciences (1R01GM106016) from the National Institutes of Health, and National Aeronautics and Space Administration (PIDDP NNX12AB16G).

REFERENCES

(1) March, R. E. *J. Mass Spectrom.* **1997**, *32*, 351−369.
(2) Ouyang, Z.; Cooks, R. G. *Annu. Rev. Anal. Chem.* **2009**, *2*, 187−214.
(3) Ouyang, Z.; Noll, R. J.; Cooks, R. G. *Anal. Chem.* **2009**, *81*, 2421−2425.
(4) Hager, J. W. *Rapid Commun. Mass Spectrom.* **2002**, *16*, 512−526.
(5) Syka, J. E. P.; Marto, J. A.; Bai, D. L.; Horning, S.; Senko, M. W.; Schwartz, J. C.; Ueberheide, B.; Garcia, B.; Busby, S.; Muratore, T.; Shabanowitz, J.; Hunt, D. F. *J. Proteome Res.* **2004**, *3*, 621−626.
(6) Makarov, A.; Denisov, E.; Lange, O.; Horning, S. *J. Am. Soc. Mass Spectrom.* **2006**, *17*, 977−982.
(7) Chernushevich, I. V.; Loboda, A. V.; Thomson, B. A. *J. Mass Spectrom.* **2001**, *36*, 849−865.
(8) Li, X. X.; Jiang, G. Y.; Luo, C.; Xu, F. X.; Wang, Y. Y.; Ding, L.; Ding, C. F. *Anal. Chem.* **2009**, *81*, 4840−4846.
(9) Maas, J. D.; Hendricks, P. I.; Ouyang, Z.; Cooks, R. G.; Chappell, W. J. *J. Microelectromech. Syst.* **2010**, *19*, 951−960.
(10) Pau, S.; Pai, C. S.; Low, Y. L.; Moxom, J.; Reilly, P. T. A.; Whitten, W. B.; Ramsey, J. M. *Phys. Rev. Lett.* **2006**, *96*; DOI: 10.1103/PhysRevLett.96.120801.
(11) Cruz, D.; Chang, J. P.; Fico, M.; Guymon, A. J.; Austin, D. E.; Blain, M. G. *Rev. Sci. Instrum.* **2007**, *78*; DOI: 10.1063/1.2403840.
(12) Misharin, A. S.; Laughlin, B. C.; Vilkov, A.; Takats, Z.; Zheng, O. Y.; Cooks, R. G. *Anal. Chem.* **2005**, *77*, 459−470.
(13) Badman, E. R.; Cooks, R. G. *Anal. Chem.* **2000**, *72*, 3291−3297.
(14) Tabert, A. M.; Goodwin, M. P.; Duncan, J. S.; Fico, C. D.; Cooks, R. G. *Anal. Chem.* **2006**, *78*, 4830−4838.
(15) Fico, M.; Maas, J. D.; Smith, S. A.; Costa, A. B.; Ouyang, Z.; Chappell, W. J.; Cooks, R. G. *Analyst* **2009**, *134*, 1338−1347.
(16) Peng, Y.; Hansen, B. J.; Quist, H.; Zhang, Z. P.; Wang, M.; Hawkins, A. R.; Austin, D. E. *Anal. Chem.* **2011**, *83*, 5578−5584.
(17) Wells, J. M.; Badman, E. R.; Cooks, R. G. *Anal. Chem.* **1998**, *70*, 438−444.
(18) Ouyang, Z.; Wu, G.; Song, Y.; Li, H.; Plass, W. R.; Cooks, R. G. *Anal. Chem.* **2004**, *76*, 4595−4605.
(19) Wu, G.; Cooks, R. G.; Ouyang, Z. *Int. J. Mass Spectrom.* **2005**, *241*, 119−132.
(20) Xu, W.; Chappell, W. J.; Ouyang, Z. *Int. J. Mass Spectrom.* **2011**, *308*, 49−55.
(21) Xu, W.; Charipar, N.; Kirleis, M. A.; Xia, Y.; Ouyang, Z. *Anal. Chem.* **2010**, *82*, 6584−6592.
(22) Gao, L.; Cooks, R. G.; Ouyang, Z. *Anal. Chem.* **2008**, *80*, 4026−4032.
(23) Chen, T. C.; Xu, W.; Garimella, S.; Ouyang, Z. *J. Mass Spectrom.* **2012**, *47*, 1466−1472.
(24) Xu, W.; Chappell, W. J.; Cooks, R. G.; Ouyang, Z. *J. Mass Spectrom.* **2009**, *44*, 353−360.
(25) Doroshenko, V. M.; Cotter, R. J. *J. Mass Spectrom.* **1997**, *32*, 602−615.

(26) He, L.; Lubman, D. M. *Rapid Commun. Mass Spectrom.* **1997**, *11*, 1467−1477.
(27) Garimella, S.; Zhou, X.; Ouyang, Z. *J. Am. Soc. Mass Spectrom.* **2013**, *24*, 1890−1899.
(28) Ouyang, Z.; Badman, E. R.; Cooks, R. G. *Rapid Commun. Mass Spectrom.* **1999**, *13*, 2444−2449.
(29) Badman, E. R.; Cooks, R. G. *Anal. Chem.* **2000**, *72*, 5079−5086.
(30) Schwartz, J. C.; Syka, J. E. P.; Quarmby, S. T. *Proceedings of the 53rd ASMS Conference on Mass Spectrometry and Allied Topics*, San Antonio, TX, June 5−9, 2005.
(31) Cunningham, C.; Glish, G. L.; Burinsky, D. J. *J. Am. Soc. Mass Spectrom.* **2006**, *17*, 81−84.
(32) Prentice, B. M.; McLuckey, S. A. *J. Am. Soc. Mass Spectrom.* **2012**, *23*, 736−744.
(33) Prentice, B. M.; Santini, R. E.; McLuckey, S. A. *J. Am. Soc. Mass Spectrom.* **2011**, *22*, 1486−1492.
(34) Prentice, B. M.; Xu, W.; Ouyang, Z.; McLuckey, S. A. *Int. J. Mass Spectrom.* **2011**, *306*, 114−122.